ELSEVIER

Journal of Pharmaceutical and Biomedical Analysis
25 (2001) 545–557

JOURNAL OF
PHARMACEUTICAL
AND BIOMEDICAL
ANALYSIS

www.elsevier.com/locate/jpba

Structural characterization of the oxidative degradation products of an antifungal agent SCH 56592 by LC–NMR and LC–MS

Wenqing Feng, Haiying Liu, Guodong Chen, Rodney Malchow, Frank Bennett, Elizabeth Lin, Birendra Pramanik, Tze-Ming Chan *

Schering-Plough Research Institute, Mail Stop: K-15-0450, 2015, Galloping Hill Road, Kenilworth, NJ 07033, USA

Received 5 September 2000; accepted 8 November 2000

Abstract

LC–NMR and LC–MS were used to characterize the structures of four major degradation products of SCH 56592, an antifungal drug candidate in clinical trials. These compounds were formed under stress conditions in which the bulk drug substance was heated in air at 150°C for 12 days, and were separated from SCH 56592 as a mixture using a semi-preparative HPLC method. The data from LC–NMR, LC–ESI–MS (electrospray ionization mass spectrometry) and LC–ESI–MS/MS indicate that the oxidation occurred at the piperazine ring in the center of the drug molecule. The structures of the degradation products were determined from the ^{1}H NMR spectra obtained via LC–NMR, which were supported by LC–ESI–MS and LC–ESI–MS/MS analyses. A novel degradation pathway of SCH 56592 was proposed based on these characterized structures.

Keywords: LC–NMR; LC–MS; Antifungal agent; Degradation

1. Introduction

SCH 56592 is a novel triazole antifungal agent that was discovered at Schering-Plough Research Institute (SPRI) [1]. Compared with the existing antifungal drugs such as amphotericin B, itraconazole and fluconazole, SCH 56592 has exhibited higher potency against a broad range of fungal pathogens including *Asperigillus*, *Candida* and *Cryptococcus* [2–6]. In particular, it was found to be most active against all species of *Aspergillus* [2,3] and it demonstrated considerable promise as a therapeutic agent in the treatment of life-threatening nosocomial fungal infections among AIDS, tissue transplant and cancer patients [for review, see [6]]. Currently, SCH 56592 is undergoing extensive clinical trials. As part of this investigation, the stability of the bulk drug substance under various conditions is being studied. At ambient conditions, the SCH 56592 drug substance is stable, but the compound begins to form degradation products under stress condi-

* Corresponding author. Tel.: +1-908-7403295; fax: +1-908-7403916.
E-mail address: tze-ming.chan@spcorp.com (T.-M. Chan).

PII: S0731-7085(00)00522-7

tions such as prolonged exposure to heat and light. In order to understand the degradation pathway, on-line liquid chromatography (HPLC) and spectroscopic methods (NMR, MS) were used for efficient identification and structural characterization of the degradation products.

LC–ESI–MS combines the high resolution separation capability of HPLC with the superior sensitivity of mass spectrometry [7]. The ESI (electrospray ionization) process provides soft ionization, and therefore generates mainly molecular ions with little fragmentation [7,8]. While LC–ESI–MS offers accurate measurement of the molecular mass, LC–ESI–MS/MS reveals structural fragmentation on each resolved molecular ion [9,10]. LC–ESI–MS and LC–ESI–MS/MS are well-established analytical tools in the rapid identification and characterization of each component in sample mixtures. However, they do not always provide unambiguous structural information and may not distinguish between isomers [11]. Nuclear magnetic resonance spectroscopy (NMR) provides detailed structural elucidation, but efficient analysis is often hindered by sensitivity and sample purity. Over the last decade, the development of LC–NMR, where the high field NMR instrument is directly coupled with the HPLC separation system, has enabled 'on-line' collection of NMR data on individual components of various chemical and biological mixtures [for review, see [12,13]]. LC–NMR allows NMR experiments conducted directly on the chromatographic resolved elution fractions, and the detection limit is lowered to less than one microgram of sample materials [14–16]. The power of LC–NMR structural determination has been successfully demonstrated on examples of drug metabolites [13–18], chemical impurities [19] and components of natural product crude extracts [20,21]. As it becomes commercially available, LC–NMR starts to be widely used in pharmaceutical industry. In practice, the results of LC–NMR in combination with LC–ESI–MS and LC–ESI–MS/MS analysis provide complementary information for rapid and unambiguous structural determination.

2. Experimental

2.1. Materials

SCH 56592 [1], (−)-4-[4-[4-[4-[[(2R-*cis*)-5-(2,4-difluorophenyl)-tetrahydro-5-(1H-1,2,4-triazol-1-ylmethyl)-3-furanyl]methoxy]phenyl]-1-piperazinyl]phenyl]-2,4-dihydro-2-[(S)-1-ethyl-2(S)-hydroxypropyl]-3H-1,2,4-triazol-3-one, was provided by the Chemical Development Group at SPRI. Two grams of SCH 56592 were weighed into an Erlenmeyer flask. The flask was covered with aluminum foil and stored in an oven maintained at 150°C for 12 days. The heat-stressed drug substance became a brown chunky mass and was ground to powder. In a similar manner, samples of the drug substance were separately subjected to near UV (UVA) fluorescent light (1×10^4 W h/m^2) and white (VIS) fluorescent light (7.6×10^6 lux-h) at room temperature. The synthetic compound SCH 57306, provided by the Discovery Research Group at SPRI, was generated by an oxidative cleavage process when SCH 56588 [1] reacted with excess chromium trioxide–pyridine complex in acetone [22]. SCH 56588 is an epimer of SCH 56592 with an *S* configuration at position C18 instead of an *R* configuration.

2.2. HPLC method for the separation of SCH 56592 and its related compounds

HPLC grade solvents were used in HPLC, LC–ESI–MS, and LC–ESI–MS/MS. Other reagents used were of analytical grade. Analytical HPLC was carried out using a reversed-phase chiral column (250 × 4.6 mm i.d., 10 mm, Chiral Technologies, Exton, PA) on a Waters 600 HPLC solvent delivery system (Waters, Milford, MA). Separations were achieved by an acetonitrile/water gradient at a flow rate of 0.75 ml/min. The column temperature was maintained at 35°C and the eluent was monitored at 254 nm. Semi-preparative HPLC was performed using a reversed-phase C8 column (250 × 20 mm i.d., 5 μm, YMC Company, Wilmington, NC) on a Rainin Dynamax Model SD-300 system. The mobile phase

contained 40% tetrahydrofuran in water. HPLC was carried out at a flow rate of 10 ml/min and ambient temperature. Fifty milligram of the stressed sample, dissolved in 1 ml of 80% acetonitrile and 20% water, was injected into the semi-preparative column. The eluent was detected at 254 nm and collected at 15 ml per fraction. The fractions were dried using a rotary evaporator and reconstituted in 3 ml of acetonitrile. One fraction was found to contain the four major degradation products and therefore was subjected to further analysis.

2.3. LC–ESI–MS and LC–ESI–MS/MS

The LC–ESI–MS and LC–ESI–MS/MS experiments were performed on a Micromass Quattro LC triple-quadrupole mass spectrometer (Manchester, UK) with a Waters Alliance 2690 system (Milford, MA) using the reversed-phase chiral column at room temperature. The water/acetonitrile gradient started from 45 to 95% acetonitrile in 25 min with 0.03% (v/v) trifluoroacetic acid added to the mobile phase. The solvent flow rate was at 1 ml/min and the flow was split post column (19:1 split) with the larger portion going to a Waters 2487 UV detector (Milford, MA) monitored at 254 nm. The smaller portion was introduced into the Micromass Quattro LC triple-quadrupole mass spectrometer. The Quattro LC system equipped with the electrospray source was used with nitrogen as the desolvation gas. The ESI voltage supplied to a stainless steel needle was 3600 V and the cone voltage was set at 10 V. The desolvation chamber was held at 300°C and the source block temperature was set at 100°C. The mass spectrometric measurement was conducted by scanning the first quadrupole mass analyzer. For MS/MS experiments, the collision gas (Ar) cell pressure was adjusted to 2.5×10^{-4} torr in order to optimize the fragmentation of the selected parent ions. The selected parent ions from the first quadrupole mass analyzer were collided with Ar in the second quadrupole with a collision energy of 60 V and the resulted product ions were obtained by scanning the third quadrupole mass analyzer.

2.4. LC–NMR

LC–NMR was performed on a Varian LC–NMR instrument (Varian Associates, Inc., Palo Alto, CA) using a Model 9012 pump system, a Model 9065 polychrome photo-diode array UV detector, an INOVA 500 MHz NMR spectrometer and a microflow LC–NMR probe. The probe has $^{1}H\{^{13}C\}$ channels with pulsed-field gradient along z axis. The active sample volume of the probe was approximately 60 μl and the transfer time from the UV cell to the active volume was calibrated to be 14 s at a flow rate of 0.75 ml/min. The HPLC separation was carried out using similar conditions as the analytical HPLC method described in Section 2.1. OmniSolv® acetonitrile (EM Science, NY) and D_2O (99.9%, Cambridge Isotope Laboratory, MA) were used as solvents. An acetonitrile/D_2O gradient was applied over 30 min. The column was kept at ambient temperature and the eluent was monitored via UV detection at 254 nm. Proton NMR experiments were performed in 'stop-flow' mode, where the HPLC flow was halted after the sample elution fraction was transferred to the LC–NMR probe which was equilibrated at 20°C. Pulse sequences WET [23,24] and WETTOCSY [24] from the Standard Varian Pulse Sequence Library were used. Double solvent suppression was applied on the proton resonances of water and acetonitrile. One-dimensional (1D) proton NMR spectra were recorded into 32 000 data points with a spectral width of 9500 Hz and 1.7 s of acquisition time. A total of 2000 transients were collected in approximately 1.5 h for each 1D proton spectrum. Two dimensional (2D) proton-proton WETTOCSY spectra were acquired using 96 scans per increment and 256 hypercomplex data points in t_1 for a total collection time of 17 h. The values for the spectral width in both F1 and F2 dimensions were set to be 8000 Hz, and the spin-lock time was 30 ms.

3. Results and discussion

The analytical HPLC chromatogram on the SCH 56592 sample is shown in Fig. 1a. SCH 56592 is displayed as the major elution peak with

a retention time of 22.3 min. At a magnified UV absorption scale, minor impurity peaks are observed across the elution process. The amount of SCH 56592 in this sample was found to be 97.9% by assaying against the SCH 56592 Reference Standard (Table 1). Therefore, the impurity content in this synthetic sample was 2.1%. Three sets of identical SCH 56592 samples were placed separately under the stress conditions including the prolonged exposure to visible light (30 days), UV light (30 days), and heat (12 days). Fig. 1b–d present the analytical HPLC chromatograms for the corresponding stressed samples. The four chromatograms (Fig. 1a–d) were recorded by injecting equal amount (5 μg) of samples under the same HPLC conditions. Compared with the control (Fig. 1a), several new peaks appeared in the chromatograms of the stressed samples (Fig. 1b–d), with the most intense signals being in the region of 11–30 min. These new peaks also had the same elution times in Fig. 1b–d. It indicated that SCH 56592 underwent degradation, and the degradation products were mainly the same under the stress of visible light, UV light and heat. The highest concentration of degradation products was found in the heat-stressed sample (Fig. 1d). The percentage of the HPLC peak area for A, B, C, D, other unidentified components and SCH 56592 are presented in Table 1. Clearly, the rate of SCH 56592 degradation appeared to be much faster under heat-stressed condition than that from exposure to light. Thus, the heat-stressed sample was selected for further structural investigation.

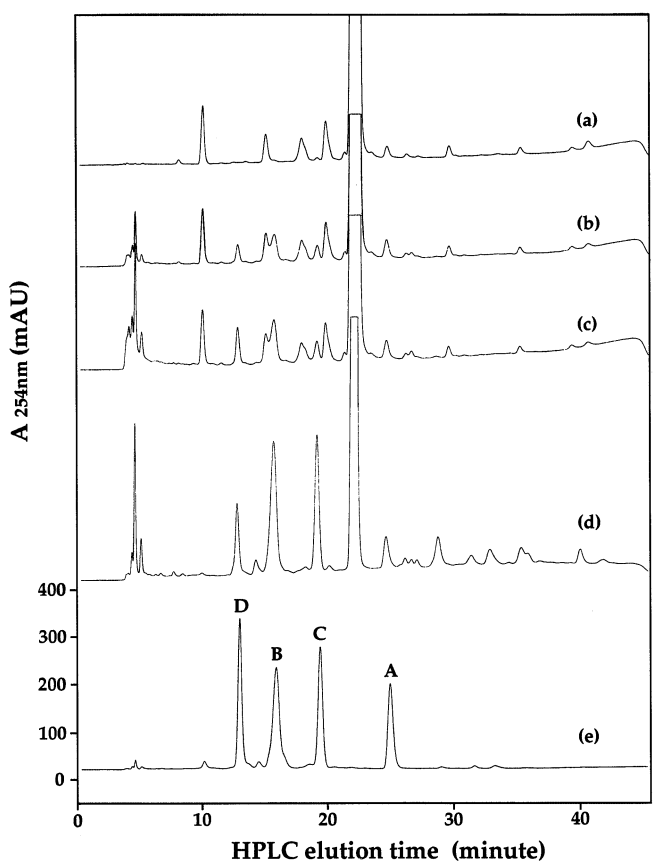

Fig. 1. HPLC–UV chromatograms of SCH 56592 (a), stressed SCH 56592 by visible light (b), UV light (c), heat (d) as well as the partially purified mixture containing the major heat-stressed degradation products of SCH 56592 (e).

Table 1
The estimation of SCH 56592 and its major degradation products and in the control and under stressed conditions

Conditions	A[a]	B[a]	C[a]	D[a]	Other[b]	SCH 56592[a]	SCH 56592[c]
Control	0.11	<0.05	<0.05	<0.05	<1.84	97.9	97.9
Visible light	0.19	0.33	0.14	0.14	2.30	96.9	95.7
UV light	0.19	0.53	0.19	0.26	3.33	95.5	93.9
Heat, 150°C	1.73	8.67	6.09	2.90	14.41	66.2	46.1

[a] The percentage of peak area is computed using the peak area of SCH 56592 divided by the total area in the HPLC chromatogram.

[b] The percentage of other unidentified components is calculated by substracting the sum of the *t* percent peak area of A, B, C, D and SCH 56592 from 100%.

[c] The percentage of the SCH 56592 amount is assayed against SCH 56592 Reference Standard.

In order to facilitate the structural studies on the degradation products that are present at less than five percent of the major components, a semi-preparative reversed-phase HPLC procedure was employed to concentrate the minor decomposed compounds and remove the interference from the major component SCH 56592. The elution fractions from the semi-preparative runs were collected and examined using the analytical HPLC method. One such fraction was found to contain four major degradation peaks at retention times of 13.0 min (D), 16.0 min (B), 19.5 min (C), and 25.0 min (A) (Fig. 1e). In addition, the parent drug substance SCH 56592 with a retention time of 22.3 min was completely removed. The fact that these four elution peaks are present in all three stressed samples (Fig. 1b–d) suggests a generalized degradation pathway. Using the peak of SCH 56592 as the reference standard, The amount of A, B, C, D and SCH 56592 was estimated by the percentage peak area in each HPLC chromatogram and the results are reported in Table 1. The amount of SCH 56592 was also assayed against SCH 56592 reference standard. Several other unidentified degradation products were observed in the chromatograms. However, except for the eluting peaks observed at 4.5 min and 29.0 min with the corresponding peak areas of 3.83 and 2.96% of the total, respectively, no other peaks exceeded the peak area of the four major degradation products A–D.

The structures of A, B, C and D were determined by LC–NMR and LC–MS, and they are shown in Fig. 2. The 1D and 2D proton NMR data for all of the chromatographic peaks were collected using LC–NMR in 'stop-flow' mode at 20°C. The downfield aromatic regions between 6.5–8.3 ppm of the proton NMR spectra for SCH 56592, A, B, C and D are plotted in Fig. 3a–e, labeled with their proton assignments. Since the mobile phase in LC–NMR was composed of acetonitrile and deuterated water, the solvent suppression on protons from HOD and CH_3^- group was achieved through the modified WET sequence [23,24]. Proton satellite peaks arising from $^{13}CH_3CN$ at natural abundance were collapsed through ^{13}C decoupling. Previously, the complete proton resonances of SCH 56592 have been assigned through the analysis of 2D COSY, HMQC, HMQC-TOCSY and HMBC experiments (unpublished data). These assignments can be transferred to the 1D spectrum of SCH 56592 (Fig. 3a) obtained by LC–NMR, despite of their minor chemical shift change in the solvent of acetonitrile/deuterium oxide. All of the proton assignments were verified by the 2D proton-proton TOCSY experiments in this work, and are listed in the following: H5″, δ 8.24, *s* (singlet); H16, δ 7.97, *s*; H3″, δ 7.73, *s*; H14, δ 7.43, *d* (doublet); H6′, δ 7.32, *m* (multiplet); H13, δ 7.13, *d*; H3′, δ 7.02, *m*; H8, δ 7.00, *d*; H5′, δ 6.89, *m*; and H7, δ 6.84, *d*. In total, there are three singlets (H3″, H5″ and H16), four doublets (H7, H8, H13 and H14), and three multiplets (H3′, H5′ and H6′). Analysis of the chemical shift change in this spectral region led to the structural elucidation of the degradation products, which are described in the following text and illustrated in Fig. 2b–e and Fig. 3b–e.

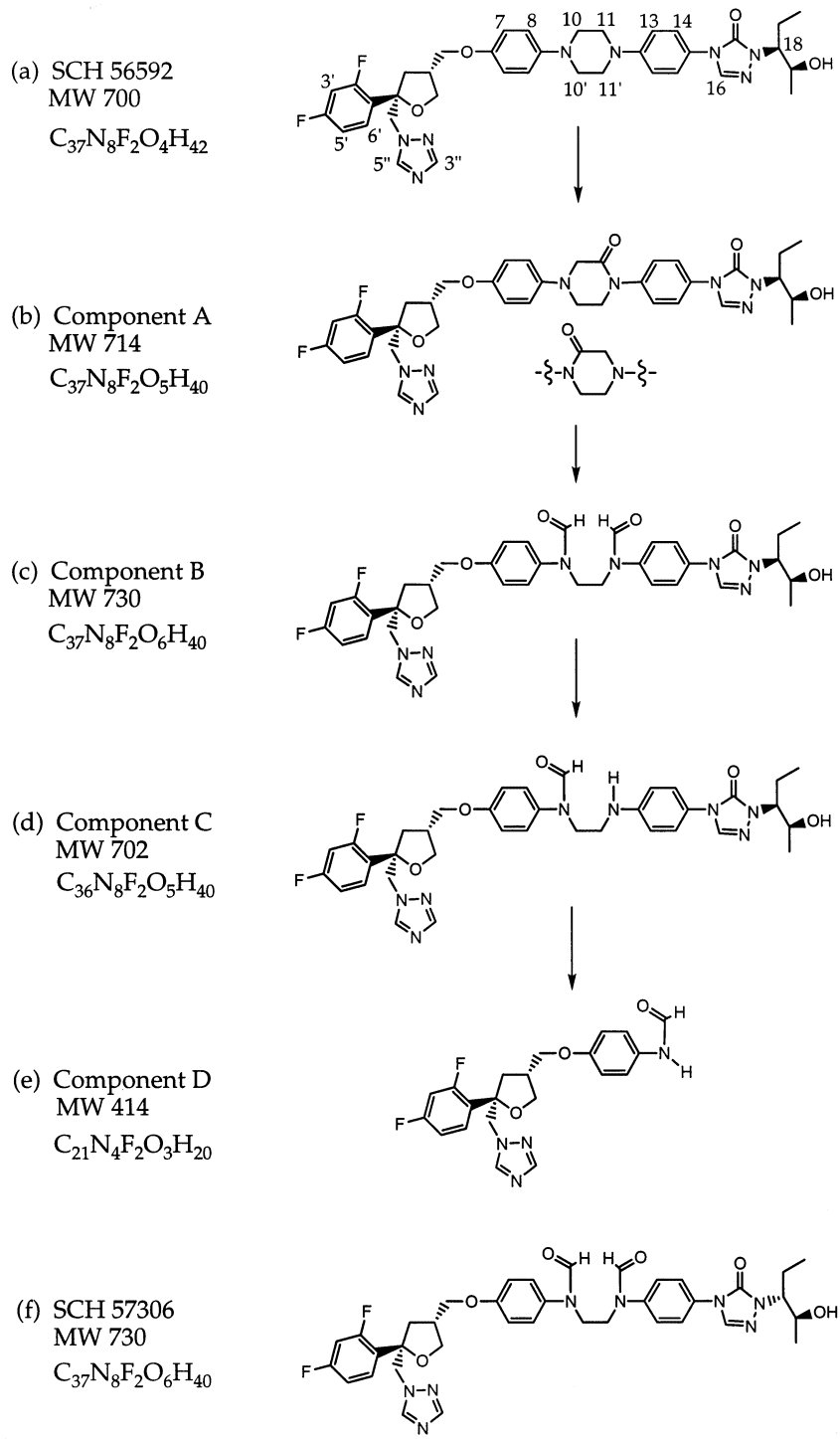

Fig. 2. The structures of SCH 56592 (a), the four major components A–D in the degradation products (b–e), and the model compound SCH 57036 (f). The proposed pathway for the oxidative degradation of SCH 56592 is outlined by vertical arrows.

LC–ESI–MS provides molecular weight information for individual components in a mixture sample under optimized electrospray conditions. It was carried out on the degradation mixture of SCH 56592 and a total ion chromatogram was obtained (Fig. 4a). Clearly, four major components A, B, C and D were observed along with several other minor components. The mass spectrum for one of the components, D, is shown in Fig. 4b. The protonated molecular ion of D was located at m/z 415, which indicated that the molecular weight of D was 414 Dalton (Da). Similarly, the molecular weight values for components A, B and C were determined to be 714, 730 and 702 Da, respectively. LC–ESI–MS/MS experiments were then carried out on these molecular ions in order to obtain their fragmentation patterns for structural analysis.

Comparing with the molecular weight 700 Da of SCH 56592, the component B (730 Da), which has an additional 30 mass units, may be the oxidized product via the addition of two oxygen atoms and the loss of two hydrogen atoms in the molecule. The major product ions from the

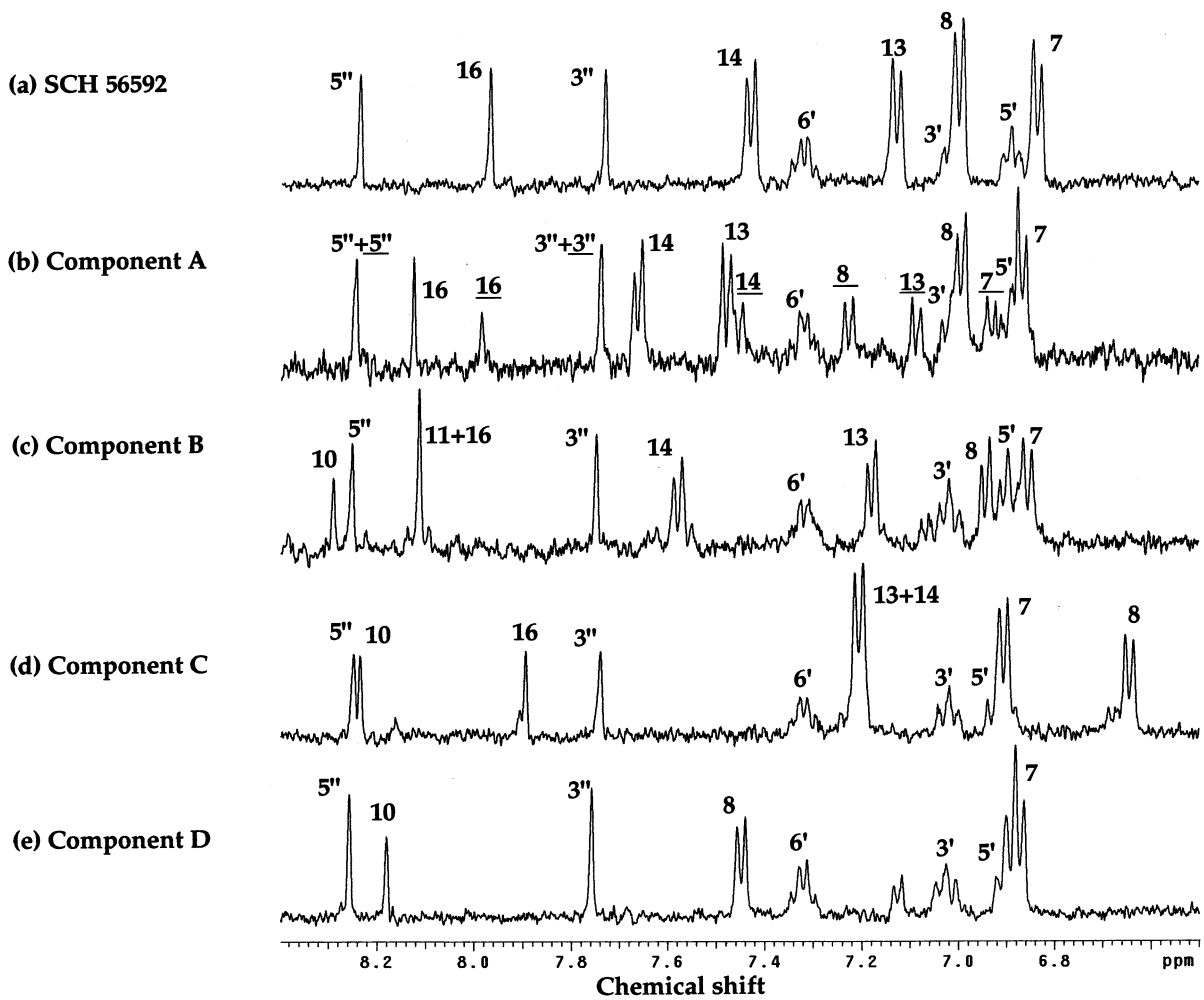

Fig. 3. The overlay of the downfield region of the ^{1}H NMR spectra for SCH 56592 (a) and its degradation components A–D (b–e). The proton assignments are labeled according to the numbering scheme shown in Fig. 3a. In the spectrum of component A (b), the proton assignments for the minor component are underlined.

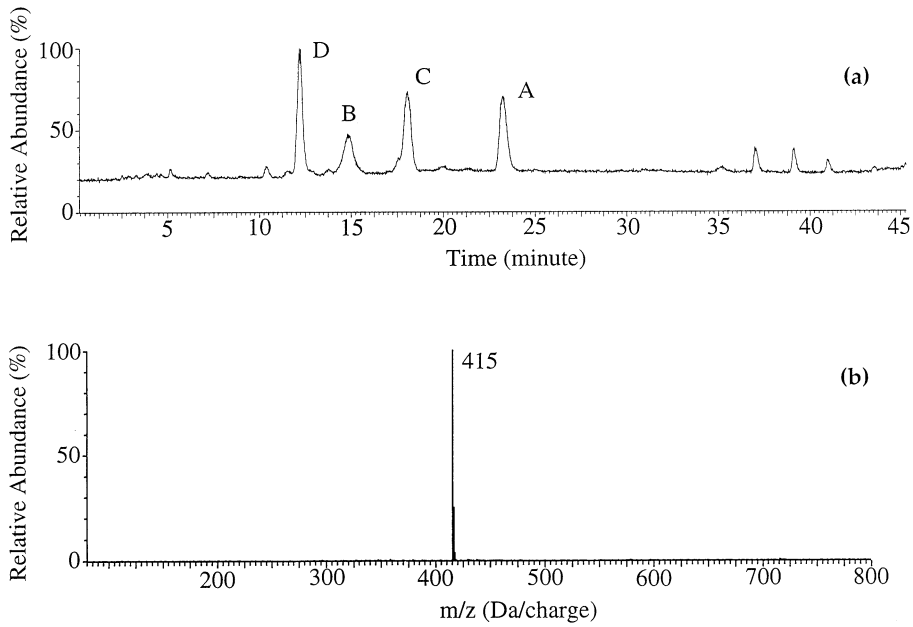

Fig. 4. The total ion chromatogram obtained from LC-ESI-MS on the partially purified mixture containing the major heat-stressed degradation products (a), and the LC–ESI–MS spectrum of component D (b).

molecular ion were detected at m/z 685, 441, 372, 317 and 299, as shown in Fig. 5a. A weak product ion was also found at m/z 703, which corresponded to the loss of a ^{-}CO group from component B. The product ion at m/z 685 was a result of the loss of a CH_3CHOH^{-} group from the molecular ion. Two major product ions at m/z 441 and 317 were observed, which is a crucial evidence for the breakdown of the center piperazine ring, as depicted in the molecular structure of B (Fig. 5a). The product ion at m/z 372 was resulted from the ion at m/z 441 after the loss of the triazole group ($^{-}C_2H_2N_3$), and the ion at m/z 299 can be readily formed from the ion at m/z 317 with the loss of H_2O. Overall, these results indicate that SCH 56592 is cleaved at the piperazine ring in the center of the molecule. The formation of NN'–formyl diamine was clearly observed in the proton NMR spectrum. In Fig. 3c of component B, two new singlets at δ 8.29 and δ 8.12 appeared, in addition to the three singlets H3″, H5″ and H16 preserved from the parent compound SCH 56592 (Fig. 3a). The singlet at δ 8.12 seems to be the overlap of a new resonance with H16, judging from the integral of this peak. The two new singlets can be assigned to formyl protons H10 and H11. In order to verify the NMR assignments, LC–NMR was carried out on a model compound (SCH 57306) under the identical HPLC conditions. SCH 57306 (Fig. 2f) is the oxidative cleavage product of SCH 56588, an epimer of SCH 56592. The chemical structure of SCH 57306 have been established by extensive NMR studies (unpublished results). Structures of SCH 56588 and SCH 56592 are identical except for a different chirality at the position C18 (Fig. 2a and f). Comparing the 1D spectra of SCH 57306, SCH 56592 and component B, the proton resonance pattern of B is identical to that of SCH 57306 in the downfield expanded region and of SCH 56592 in the aliphatic region. Thus the formyl protons H10 and H11 can be assigned based on their chemical shifts in the standard compound SCH 57306. And the structure of B is identified as the epimer of SCH 57306 (Fig. 2f).

Component C (molecular weight 702 Da) corresponded to a product of B (MW 731 Da) generated by the loss of a carbonyl group (^{-}CO).

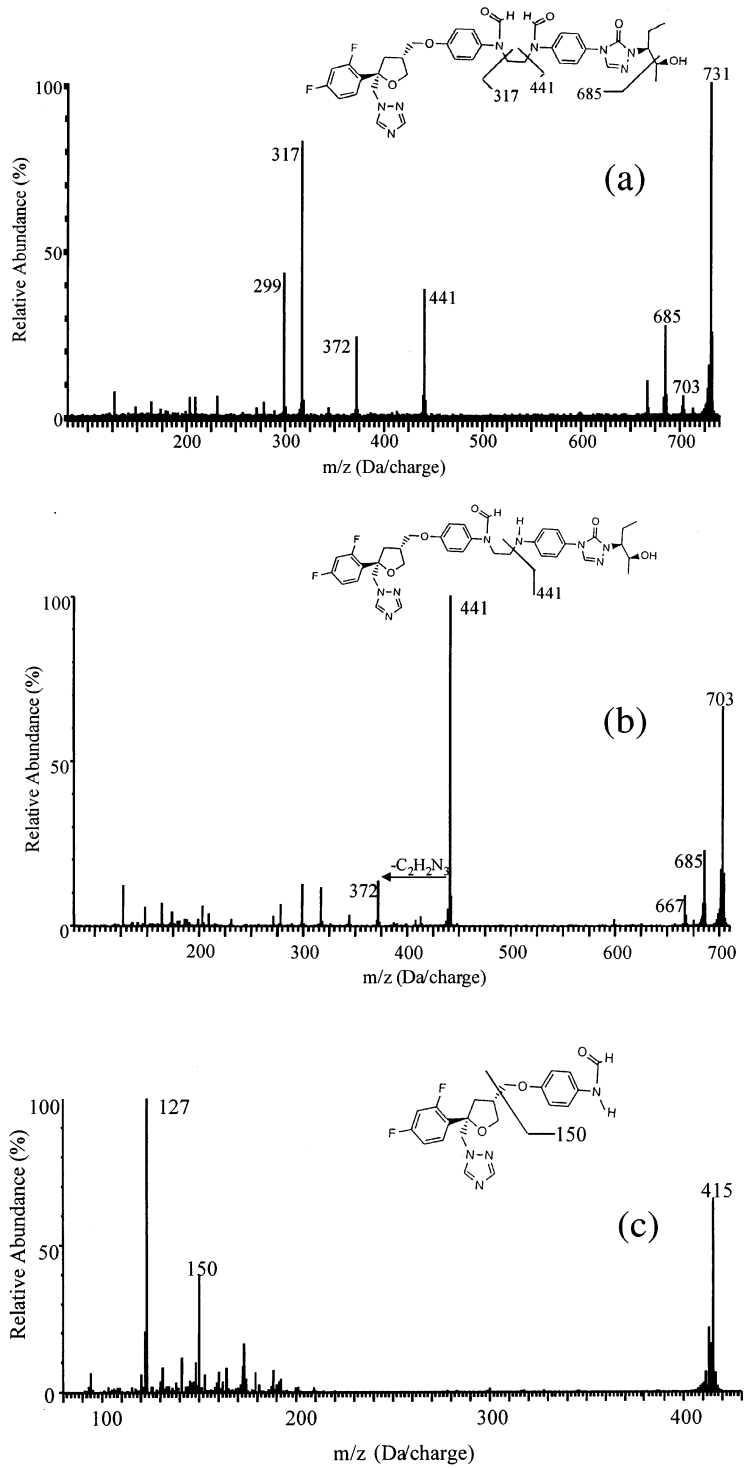

Fig. 5. MS/MS product ion mass spectrum of the protonated molecular ions at m/z 731 (a), 703 (b) and 415 (c) for components B, C and D, respectively.

LC–ESI–MS/MS experiments on the protonated molecular ion at m/z 703 yielded a strong product ion at m/z 441 and a weak one at m/z 372 (Fig. 5b). In addition, the consecutive loss of H_2O from the parent molecular ion yielded the product ions at m/z 685 and 667. Similar to component B, the product ion at m/z 372 was generated from the fragmentation of ions at m/z 441 via a loss of the $^{-}C_2H_2N_3$ group. Therefore it is proposed the formyl group at C11 in component B is absence in C, which is consistent with the NMR data. In the NMR spectrum of component C (Fig. 3d), a new singlet was observed in addition to the three singlets H3″, H5″ H16 (Fig. 3a and Fig. 3d). Comparing with the singlets in Fig. 3c of component B, this new singlet can be assigned to formyl proton H10, but another formyl proton H11 in B was not found. The disappearance of H11 suggests that the deformylation occurred at C11. In total, both MS and NMR analysis support the structure of component C as shown in Fig. 2d.

The component D generated a protonated molecular ion at m/z 415 by LC–ESI–MS, indicating a breakdown of the SCH 56592 molecule. The MS/MS product ion spectrum showed product ions at m/z 127 and 150 (Fig. 5c). The most intense product ion at m/z 127 was likely a stable di-fluoro benzonium ion. The evidence from NMR clearly points to the cleavage at the covalent bond C10′–C11′ (Fig. 3e). The presence of the singlet resonances H5″ H10, and H3″ plus the disappearance of H16, H13 and H14 strongly support the structure shown in Fig. 2e for component D.

For component A, the molecular ion was found to be a homogenous peak and the molecular weight was determined to be 714 Da from LC–ESI–MS analysis. The MS/MS data exhibited very limited product ions for structural characterization (data not shown). The mass unit of compound A was 14 mass units more than SCH 56592, which suggests that one oxygen atom is added with the removal of two hydrogen atoms on SCH 56592. Interestingly, comparing the NMR spectra of component A (Fig. 3b) and SCH 56592 (Fig. 3a), the numbers of the singlets and doublets in A are doubled (a major and a minor set), indicating the presence of two compounds. The purity of each HPLC peak fraction can also be estimated by the convergence of its UV absorption profiles across the elution peak of interest, assuming the retention times and peak shapes are not identical for all components. The UV absorption profile is collected at every elution time point by the polychrome detector and readily available after each HPLC run. Fig. 6a shows the expansion of the HPLC chromatogram covering peaks for components C and A. Six points are marked before and after the peak apexes (Fig. 6a) and their UV absorption profiles are displayed in Fig. 6b. The profiles at points 1 (located at the first half of peak C) and 2 (located at the second half of peak C) form an indiscernible bundle. Whereas those taken at the first half of peak A (points 3 and 4) seem to be characteristically different from

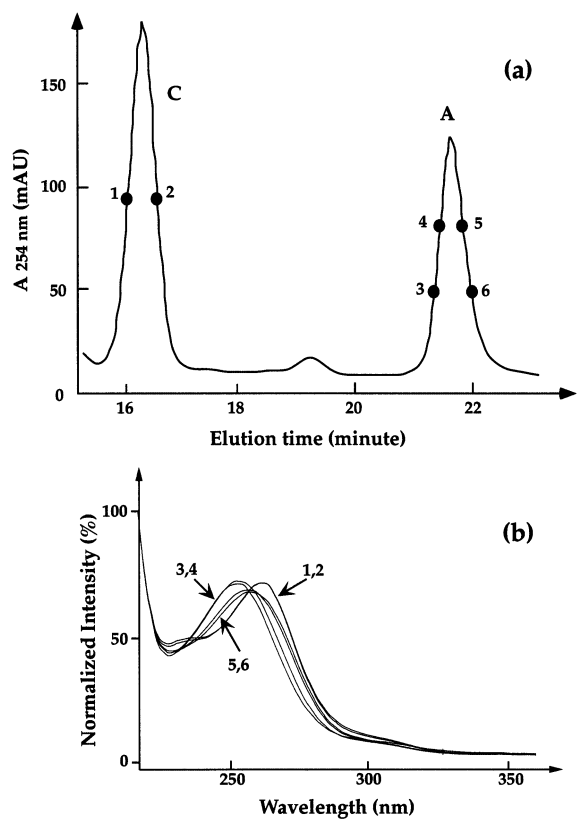

Fig. 6. The expansion of the HPLC chromatogram containing the elution of components C and A (a). The UV absorption scanning profiles from 210 to 330 nm are shown in (b) for elution time points 1–6 in (a).

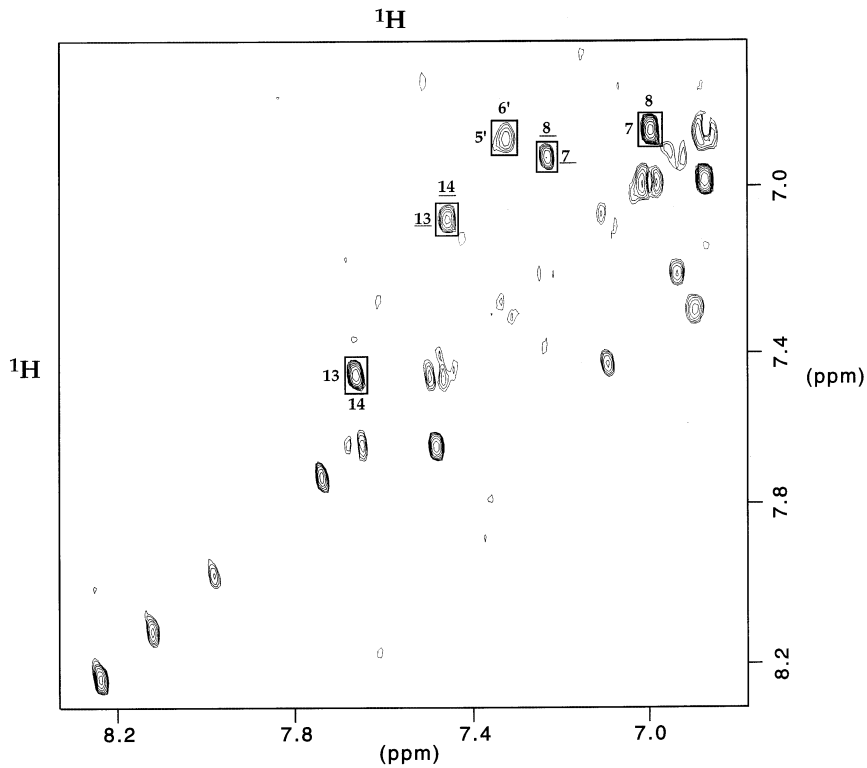

Fig. 7. The aromatic region of the 2D proton-proton TOCSY spectrum collected on component A in stop-flow mode. The cross peaks arising from the minor component in A are underlined.

the ones at the second half of peak A (points 5 and 6). Furthermore, the absorption maxim was found to be 226.7 nm for points 3 and 4, but it was 230.7 nm for points 5 and 6. These absorption data suggest that peak C was composed of a pure component and peak A contained more than one component. In order to confirm this point, 2D proton-proton TOCSY data was recorded on the elution peak A using LC–NMR in the stop-flow mode, and the aromatic spectral region is plotted in Fig. 7. In this TOCSY spectrum, five cross peaks were observed, of which two sets for H13–H14 and H7–H8 correlation, respectively. The cross peaks arising from the minor conformation are underlined in Fig. 7. In addition, their chemical shifts were consistent with the fact that a tertiary amine was converted to a secondary amide group. In the major component, the chemical shifts of H13 and H14 (7.13 and 7.43 ppm) were shifted downfield (7.46 and 7.66 ppm) while H7 and H8 remained. In the minor component, H13 and H14 remained, while H7 and H8 (6.86 and 6.98 ppm) were shifted downfield (6.94 and 7.23 ppm). These shifts were consistent with the oxidation occurring at position C11 in the major form and position C10 in the minor form. Combining these analyses, component A is consisted of two structural isomers and their structures are presented in Fig. 2b.

The formation of formyl analogs from secondary and tertiary amines has previously been reported in the literature [22,25]. For example, the oxidation of substituted ethylenediamines in the presence of manganese dioxide gives *N*-formyl compounds [22]. Based on the stable structures determined from this study, we propose the oxidative degradation pathway of SCH 56592 as follows. The air oxidation of SCH 56592 initially yields a mixture of oxidation products at C10 or C11 positions, represented by the two structures

in component A (Fig. 2b). Further oxidation at both C10 and C11 leads to the formation of *N N′*–diformyl structure in B (Fig. 2c). Deformylation of B forms C with one *N*-formyl group remained and one secondary amine (Fig. 2d). Subsequent oxidative cleavage causes the breakdown of the structure C into D (Fig. 2e). Since there are other minor peaks existing in the HPLC elution of the stressed drug substance (Fig. 1b–d) that are not identified in this study, other degradation products may be present. However, the proposed oxidative degradation pathway is believed to be the dominant one for the three stress conditions studied, and it provides the basis for further stability evaluation of this novel antifungal agent.

4. Conclusions

This work demonstrates the practical utility of LC–NMR, LC–ESI–MS and LC–ESI–MS/MS in the efficient structural elucidation of the novel degradation products of bulk drug substance SCH 56592. In general, at this stage of the stability investigation, many analogs of the drug molecule are available as model compounds for structural studies. Online combination of these analytical tools (HPLC, NMR and MS) brings superior efficiency to their uncoupled use in the identification and structural determination of individual chemical components in the complex mixtures. The feasibility of physically linking these systems, such as LC–NMR–MS, where high field NMR and electrospray MS spectrometers are connected parallel after the HPLC system, has been successfully demonstrated in the structural analysis of chemical mixtures and metabolites in biological fluids [26–29]. As the commercial systems become available, LC–NMR–MS will be increasingly popular in the areas where the sample amount and purity present a challenge.

Acknowledgements

The authors would like to thank Drs P. Weber and D. Chambers for helpful comments on the manuscript, and J. Colby for technical assistance.

References

[1] V.M. Girjiavallabhan, A.K. Saksena, R.G. Lovey, F. Bennett, R.E. Pike, H. Wang, P. Pinto, Y.T. Liu, N. Patel, A.K. Ganguly, 35th Interscience Conference on Antimicrobial Agents and Chemotherapy (ICAAC), San Francisco, California, September 17–20, 1995, Abstract No. F61.
[2] R. Parmegiani, A. Cacciapuoti, D. Loebenberg, B. Antonacci, C. Norris, T. Yarosh-Tomaine, M. Michalski, R.S. Hare, G.H. Miller, 35th Interscience Conference on Antimicrobial Agents and Chemotherapy (ICAAC), San Francisco, California, September 17–20, 1995, Abstract No. F62.
[3] K.L. Oakley, C.B. Moore, D.W. Denning, Antimicrob. Agents Chemother. 41 (1997) 1124–1126.
[4] D. Law, C.B. Moore, D.W. Denning, Antimicrob. Agents Chemother. 41 (1997) 2310–2311.
[5] J.R. Perfect, G.M. Cox, R.K. Dodge, M.A. Schell, Antimicrob. Agents Chemother. 40 (1996) 1910–1913.
[6] Y. Koltin, C.A. Hitchcock, Curr. Opin. Chem. Biol. 1 (1998) 176–182.
[7] W.M.A. Niessen, J. Chromatogr. A. 794 (1998) 407–435.
[8] J.B. Fenn, M. Mann, C.K. Meng, S.F. Wong, C.M. Whitehouse, Science 246 (1989) 64–71.
[9] K.L. Busch, G.L. Glish, S.A. McLuckey, Mass Spectrometry/Mass Spectrometry: Techniques and Applications of Tandem Mass Spectrometry, VCH Publishers, Inc., New York, 1988.
[10] B. Pramanik, P.L. Bartner, G. Chen, Curr. Opin. Drug Discov. Develop. 2 (1999) 401–417.
[11] J. Chin, J.B. Fell, M. Jarosinski, M.J. Shapiro, J.R. Wareing, J. Org. Chem. 63 (1998) 386–390.
[12] J.C. Lindon, J.K. Nicholson, I.D. Wilson, Adv. Chromatogr. 63 (1995) 315–382.
[13] J.C. Lindon, J.K. Nicholson, U.G. Sidelmann, I.D. Wilson, Drug Metab. Rev. 29 (1997) 705–746.
[14] M. Spraul, M. Hofmann, P. Dvortsak, J.K. Nicholson, I.D. Wilson, Anal. Chem. 65 (1993) 327–330.
[15] J.P. Shockcor, R.M. Wurm, L.W. Frick, P.N. Sanderson, R.D. Farrant, B.C. Sweatman, J.C. Lindon, Xenobiotica 26 (1996) 189–199.
[16] W.J. Ehlhardt, J.M. Woodland, T.M. Baughman, M. Vandenbranden, S.A. Wrighton, J.S. Kroin, B.H. Norman, S.R. Maple, Drug Metab. Dispos. 26 (1998) 42–51.
[17] J.P. Shocker, I.S. Silver, R.M. Wurm, P.N. Sanderson, R.D. Farrant, B.C. Sweatman, J.C. Lindon, Xenobiotica 26 (1996) 41–48.
[18] E.M. Lenz, D. Greatbanks, I.D. Wilson, M. Spraul, M. Hofmann, J. Troke, J.C. Lindon, J.K. Nicholson, Anal. Chem. 68 (1996) 2832–2837.

[19] J.K. Roberts, R.J. Smith, J. Chromatogr. A. 677 (1994) 385–389.
[20] O. Spring, H. Buschmann, B. Vogler, E.E. Schilling, M. Spraul, M. Hoffmann, Phytochemistry 39 (1995) 609–612.
[21] B. Vogler, I. Klaiber, G. Roos, C.U. Walter, W. Hiller, P. Sandor, W. Kraus, J. Natural Prod. 61 (1998) 175–178.
[22] E.F. Curragh, H.B. Henbest, A. Thomas, J. Chem. Soc. (1960) 3559–3563.
[23] R.J. Ogg, P.B. Kingsley, J.S. Taylor, J. Magn. Reson. Ser. B. 104 (1994) 1–10.
[24] S.H. Smallcombe, S.L. Patt, P.A. Keifer, J. Magn. Reson. Ser. A. 117 (1995) 295–303.
[25] H.B. Henbest, M.J. Stratford, J. Chem. Soc. (C) (1966) 995–996.
[26] F.S. Pullen, A.G. Swanson, M.J. Newman, D.S. Richards, Rapid Commun. Mass Spectrom. 9 (1995) 1003–1006.
[27] J.P. Shockcor, S.E. Unger, I.D. Wilson, P.J.D. Foxall, J.K. Nicholson, J.C. Lindon, Anal. Chem. 68 (1996) 4431–4435.
[28] K.I. Burton, J.R. Everett, M.J. Newman, F.S. Pullen, D.S. Richards, A.G. Swanson, J. Pharm. Biomed. Anal. 15 (1997) 1903–1912.
[29] R.M. Holt, M.J. Newman, F.S. Pullen, D.S. Richards, A.G. Swanson, J. Mass Spectrom. 32 (1997) 64–70.